Available online at www.sciencedirect.com
ScienceDirect
Ceramics International 35 (2009) 289–293
CERAMICS INTERNATIONAL
www.elsevier.com/locate/ceramint

Crystallographic characterization of silicon nitride ceramics sintered with Y_2O_3–Al_2O_3 or E_2O_3–Al_2O_3 additions

C. Santos [a,*], S. Ribeiro [a], K. Strecker [a], P.A. Suzuki [a], S. Kycia [b,1], C.R.M. Silva [c]

[a] *Universidade de São Paulo-Escola de Engenharia de Lorena (USP-EEL), Brazil*
[b] *Laboratório Nacional de Luz Síncrotron (LNLS), Brazil*
[c] *Centro Técnico Aeroespacial, Divisão de Materiais (CTA-IAE-AMR), Brazil*

Received 27 August 2007; received in revised form 10 September 2007; accepted 10 October 2007
Available online 8 December 2007

Abstract

Silicon nitride ceramics were sintered using Y_2O_3–Al_2O_3 or E_2O_3–Al_2O_3 (E_2O_3 denotes a mixed oxide of Y_2O_3 and rare-earth oxides) as sintering additives. The intergranular phases formed after sintering was investigated using high-resolution X-ray diffraction (HRXRD). The use of synchrotron radiation enabled high angular resolution and a high signal to background ratio. Besides the appearance of β-Si_3N_4 phase the intergranular phases $Y_3Al_5O_{12}$ (YAG) and Y_2SiO_5 were identified in both samples. The refinement of the structural parameters by the Rietveld method indicated similar crystalline structure of β-Si_3N_4 for both systems used as sintering additive. On the other hand, the intergranular phases $Y_3Al_5O_{12}$ and Y_2SiO_5 shown a decrease of the lattice parameters, when E_2O_3 was used as additive, indicating the formation of solid solutions of $E_3Al_5O_{12}$ and E_2SiO_5, respectively.

Keywords: D. Si_3N_4; $Y_3Al_5O_{12}$; Y_2SiO_5; X-ray diffraction; Rietveld method

1. Introduction

Silicon nitride ceramics have been intensively investigated, due to its elevated thermo-mechanical properties such as creep, corrosion and oxidation resistance [1,2]. One of the difficulties found in the fabrication process is the sintering to attain high relative densities. Therefore, the use of additives to form a liquid phase and to promote densification by particle rearrangement and solution-precipitation processes is required. On the other hand, the additives form a secondary intergranular glassy phase after sintering, which decrease the high-temperature properties of these materials. The crystallization of these additives into refractory phases may reduce this problem [1–3].

The additive systems mostly employed to the sintering of Si_3N_4 are: AlN–Y_2O_3 and Al_2O_3–SiO_2, for the formation of SiAlONs or solid solutions of Si_3N_4 [1,4,5]. Additive systems of Y_2O_3–SiO_2 and Al_2O_3–Y_2O_3 are also used in several molar fractions and may be crystallized into phases such as: Y_2SiO_5, Y_2SiO_7, $YSiO_2N$, $Y_2Si_3N_4O_3$ (mellilite) or $Y_3Al_5O_{12}$ (YAG – yttrium aluminum garnet) by an appropriate heat treatment after sintering. These crystalline phases exhibit good mechanical properties and a high crack propagation resistance, which contribute to increase the fracture toughness of the sintered ceramics [1,6].

It has been shown in previous works [7–10] that the mixed oxide, E_2O_3, composed by yttrium and rare-earth oxides, is a potential substitute for pure Y_2O_3 to the sintering of Si_3N_4 ceramics, resulting in materials with similar physical, chemical and mechanical properties. It has also been found that the mixed oxide is a solid solution composed mainly by Y_2O_3 (44 wt.%), Yb_2O_3 (17 wt.%), Er_2O_3 (14 wt.%) and Dy_2O_3 (11 wt.%) and other rare-earth oxides in fractions smaller than 3 wt.%. The mixed oxide crystallizes in a Y_2O_3-type structure [10].

Recently, the mechanical properties of Si_3N_4–ceramics sintered with Al_2O_3–Y_2O_3 or Al_2O_3–E_2O_3 additions have been investigated [9]. The results of the both ceramic materials

* Corresponding author. Tel.: +55 12 31599915; fax: +55 12 31533006.
E-mail address: claudinei@demar.faenquil.br (C. Santos).
[1] Present address: University of Gwelph, Physics Department, Gwelph, Canada.

0272-8842/$34.00
doi:10.1016/j.ceramint.2007.10.014

prepared using these additives were quite similar in terms of densification, microstructure and mechanical properties, such as hardness, flexural strength and fracture toughness. For the α-SiAlONs prepared using these additives, similar characteristics of microstructure and mechanical behavior were detected in the materials prepared with Al_2O_3–Y_2O_3 or Al_2O_3–E_2O_3 [8,10].

The aim of this work was the investigation of the crystalline intergranular phases formed into Si_3N_4 ceramics sintered with Al_2O_3–Y_2O_3 or Al_2O_3–E_2O_3 mixtures as additives. These analyses were carried out using high-resolution X-ray diffractometry with synchrotron light as source. This setup provides a high-resolution determination of lattice parameters and a high intensity of the X-rays into the samples. These characteristics allow the investigation of small variations in the crystal structures of Si_3N_4 due to the incorporation of Al^{3+} or O^{2-} ions from the additives and also the detection of small amounts of intergranular phases.

2. Experimental procedure

2.1. Sample preparation

For the preparation of the powder batches, α-Si_3N_4 (UBE Industries, E-10), α-Al_2O_3 (Baikalox, 99.9%), Y_2O_3 (H.C. Starck, 99.98%) and E_2O_3 (DEMAR-FAENQUIL, 99.98%) powders were used. The batches were prepared by mixture of 86 vol.% Si_3N_4 and 14 vol.% of the following additive mixtures: Y_2O_3–Al_2O_3 (SNYA sample) or E_2O_3–Al_2O_3 (SNEA sample). The fraction of the additives was calculated to form $Y_3Al_5O_{12}$ as intergranular phase, namely, 40 mol% of Y_2O_3 (or E_2O_3) and 60 mol% of Al_2O_3. The compositions of the prepared powder batches in wt.% are listed in Table 1. The different weight-percentage of the additives used are due to the different densities of Y_2O_3 (5.01 g cm^{-3}) and E_2O_3 (6.51 g cm^{-3}), as determined by He-picnometry.

The batches were prepared by ball-milling at 500 rpm for 6 h in isopropilic alcohol. The suspension was dried in a rotary evaporator and the put inside an oven at 100 °C for 24 h. After drying, the powders were sieved for deagglomeration. Green bodies were prepared by uniaxial pressing in a steel die (50 MPa) and isostatic pressing under 300 MPa.

Sintering of the samples was done in a furnace with graphite resistance putting on a graphite crucible with a powder bed composed of Si_3N_4 (70 wt.%) and BN (30 wt.%) powders. The samples were heated with a rate of 10 °C/min up to 1900 °C in 1.5 MPa nitrogen atmosphere. The soaking time was 2 h at 1900 °C. In order to crystallize the intergranular glassy phase, the samples were heat-treated at 1400 °C for 24 h under 0.1 MPa nitrogen atmosphere [11].

The density of the samples was determined by the immersion method in distilled water, according to the Archimedes' principle.

2.2. Phases analysis

For each compound, three sintered samples were crushed into powders and homogenized, for high-resolution X-ray diffraction (HRXRD) analysis. The powders were sieved to select particles smaller than 20 μm. The analyses were done at the Brazilian Synchrotron Light Laboratory (LNLS) at Campinas-Brazil, using the XRD1-D12A beamline. A Hubber diffractometer with multiple-axis was used. The measurements were conducted with a configuration of two coupled concentric circles (ω–2θ), using a monochromatic beam of 10 keV (λ = 1.2398 Å) energy. The powders were carefully pulverized on a sample holder and it was rotated to improve the random orientation of the crystalline planes. The diffracted beam was collected using a (2 0 0) oriented Ge analyzer crystal and scintillation detector. The patterns were obtained at room temperature in q-space ($q = 4\pi\lambda^{-1} \sin\theta = d^{-1}$) in order to optimize the number of points for each peak. The data were collected in the interval of $0.50 \leq q \leq 6.50$, with 0.01 steps using 1 s of counting time. After the data acquisition, q was converted to 2θ. For each compound 2 measurements were conducted, to guarantee reproducibility of the analysis; the standard deviation of the calculated lattice parameters has been smaller than 0.007 Å, see Table 2.

The simulations of the diffractograms were performed using the Powdercell software [12]. The structural parameters as lattice parameters and atomic positions of the crystal structures were refined by the Rietveld method using the FullProf computer program [13].

2.3. Microstructure

The microstructure of the sintered samples was observed by scanning electron microscopy (*SEM LEO-1450VP*, *England*) equipment with secondary electron detector. The samples were cut and polished. The surface of the samples was plasma-etched.

The grain size distribution and the aspect ratio were determined by the method proposed by Wötting et al. [14], which is based on the measurements of the length and width of 10% of the largest grains observed in the cross-section analyzed.

Table 1
Composition of the samples

Composition	(In wt.%)			
	Si_3N_4	Al_2O_3	Y_2O_3	E_2O_3
SNYA (86 vol% Si_3N_4 + 14 vol%Y_2O_3–Al_2O_3)	81.4	8.0	10.6	–
SNEA (86 vol% Si_3N_4 + 14 vol% E_2O_3–Al_2O_3)	78.8	7.6	–	13.6

Table 2
Lattice parameters and volume of Y_2SiO_5 and E_2SiO_5

	Y_2SiO_5 (SNYA)	E_2SiO_5 (SNCA)
a (Å)	12.439(7)	12.408(8)
b (Å)	6.751(5)	6.733(4)
c (Å)	10.414(7)	10.395(7)
β (°)	102.65(5)	102.63(5)
V (Å^3)	853.3(9)	847.3(9)

The number in the parenthesis denotes standard deviation.

3. Results and discussion

3.1. Materials characterization

The relative density of the silicon nitride ceramics prepared using Y_2O_3–Al_2O_3 as additive (SNYA) and E_2O_3–Al_2O_3 as additive (SNEA) after sintering was found to be near 99.5% of the theoretical density for both samples. Furthermore, both materials exhibited similar mechanical properties, as hardness of 13 GPa, flexural strength around 680 MPa and fracture toughness of 6.7 MPa $m^{1/2}$ [9].

3.2. Phase analysis

The X-ray diffraction patterns of SNYA and SNEA samples after sintering are shown in Fig. 1(a) and (b), respectively. In both diffractograms, narrow and well-defined peaks are present, indicating crystalline phases. The predominant matrix phase is constituted by β-Si_3N_4, as can be verified by comparison with the simulated diffraction pattern of pure β-Si_3N_4, shown in Fig. 1(c). Further low intensity diffraction peaks were attributed to the crystalline intergranular phases.

The refinement of the lattice parameters of the β-Si_3N_4 phase was done using the Rietveld method, based on the literature data: hexagonal system, space group $P6_3$, $a = 7.595(1)$Å and $c = 2.9023(6)$Å, and the atomic positions according to Grün [15]. The refined lattice parameters for the β-Si_3N_4 phase were: $a = 7.6093(5)$Å and $c = 2.9134(3)$Å for the SNYA sample and $a = 7.6063(7)$Å and $c = 2.9124(5)$Å for the SNEA sample. These values, slightly higher than that reported in the literature indicate a possible dissolution of small amount of Al^{3+} and/or O^{2-} of the additives into the Si_3N_4 structure. The refined atomic positions for both samples SNYA and SNEA were very close to the reported values. Thus, the structure of β-Si_3N_4 for both samples studied, SNYA and SNEA, were similar, indicating that the different additives used, e.g. respectively Y_2O_3–Al_2O_3 and E_2O_3–Al_2O_3 lead to similar materials.

The intergranular phases were identified by expanding the *y*-axis of the X-ray diffraction patterns, as can be see in the Fig. 2.

Two intergranular crystalline phases have been identified: $Y_3Al_5O_{12}$ (YAG) and Y_2SiO_5. The Y_2SiO_5 phase, not expected, could be formed by the reaction of SiO_2, inherently present on the surface of the Si_3N_4 particles, and Y_2O_3. It should be mentioned that all diffraction peaks, belonging to β-Si_3N_4, as to the intergranular phases appear in the both materials prepared, indicating that the same phases have been formed, independently of the additive system employed, Al_2O_3–Y_2O_3 (SNYA) or Al_2O_3–E_2O_3 (SNEA).

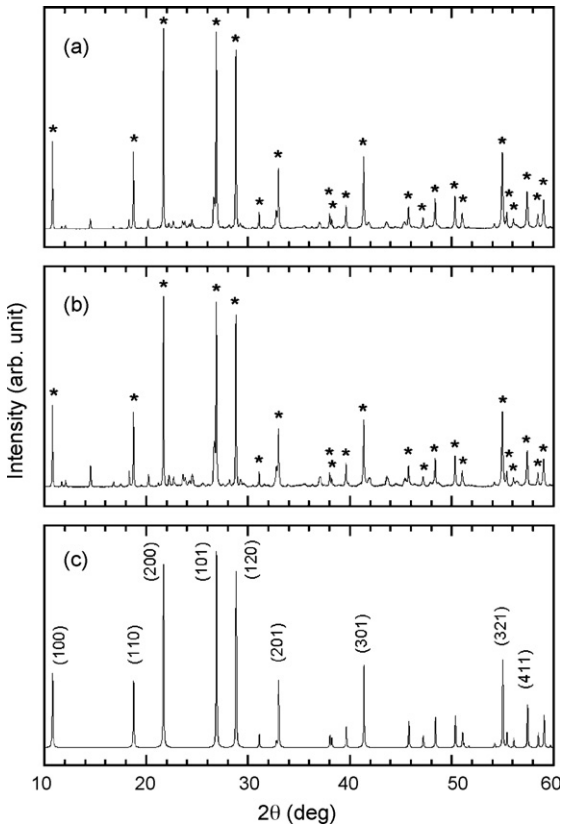

Fig. 1. X-ray diffractograms of (a) SNYA and (b) SNEA samples. In (c) a simulation of β-Si_3N_4 phase is shown. The symbol (*) indicates the peaks belonging to β-Si_3N_4 phase.

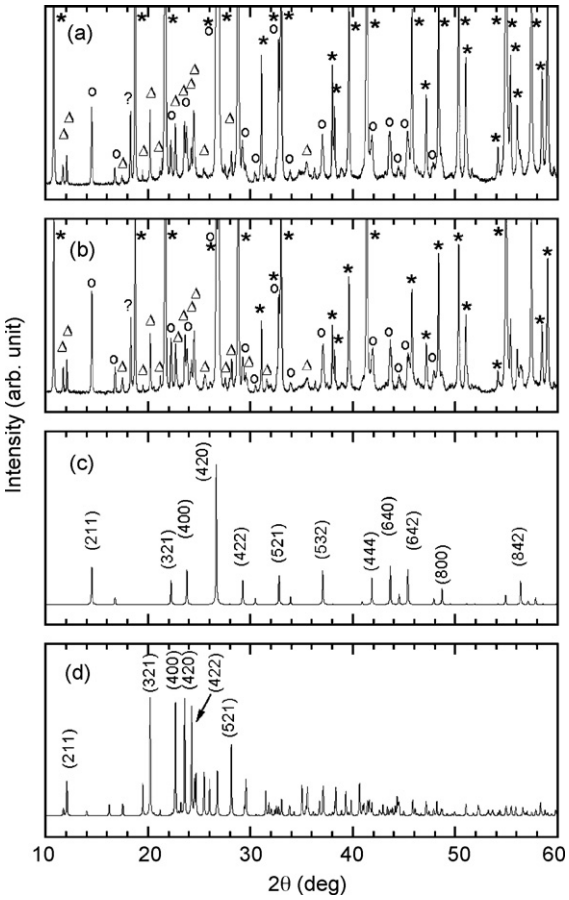

Fig. 2. Expanded X-ray diffractograms of (a) SNYA and (b) SNEA samples. In (c) and (d) simulation of $Y_3Al_5O_{12}$ and Y_2SiO_5 phases are shown, respectively. The peaks were identified by the symbols (*): β-Si_3N_4, (o): $Y_3Al_5O_{12}$ and (Δ): Y_2SiO_5.

The structural parameters of the $Y_3Al_5O_{12}$ phase were refined by the Rietveld method, based on the literature data: cubic structure, space group *I*a3*d*, $a = 12.000$ Å, and the atomic positions according to Euler and Bruce [16]. The lattice parameters determined by the refinement were: $a = 12.023(3)$Å for SNYA and $a = 12.004(3)$Å for SNEA. The lattice parameter of this phase shown a slight variation, depending on the additive system used. The decrease of 0.02 Å in the lattice parameter of the YAG phase in the SNEA sample in comparison to that of SNYA sample indicates the formation of a solid solution, $E_3Al_5O_{12}$. This interpretation is supported by the difference found in the smaller lattice parameter of the solid solution E_2O_3 ($a = 10.588(1)$Å) when compared to that of the pure Y_2O_3 ($a = 10.6080(1)$Å) [10]. The refinement of the oxygen atomic positions of $Y_3Al_5O_{12}$ in SNYA and SNEA samples were almost unchanged, presenting values very close to the reported ones.

The appearance of Y_2SiO_5 phase in both samples was confirmed by the comparison to the JCPDS-ICDD files (36–1476) [17]. There are known two polymorphs for RE_2SiO_5 phase (RE = Y or rare-earth atom) [18]: the so-called X_1 phase (monoclinic, space group $P2_1/c$), stable at room temperature for RE = La to Gd and X_2 phase (monoclinic, space group C2/c), stable at room temperature for RE = Dy to Lu. They are also known as high-temperature phase (X_1 phase) and low-temperature phase (X_2 phase). The Y_2SiO_5 phase appearing in both samples SNYA and SNEA was identified to exhibit the X_2-type structure.

The crystal structure of the X_1 phase has been recently investigated by Wang et al. [18]. On the other hand, very few data about the X_2 phase are available in the literature. The lattice parameters for the Y_2SiO_5 phase were reported in JCPDS-ICDD file (36–1476) [17]: $a = 12.50$ Å, $b = 6.728$ Å, $c = 10.42$ Å and $\beta = 102.68^\circ$. The initial atomic positions for the refinement of the Y_2SiO_5 phase were based on the data of Lu_2SiO_5 phase reported by Gustafsson [19], since no data were found for Y_2SiO_5 and also based on a similar monoclinic symmetry for both compounds. Thus, the refined lattice parameters and unit cell volume ($Z = 8$) for Y_2SiO_5 are shown in Table 2. Note that the lattice parameters for E_2SiO_5 phase in the SNEA sample are smaller than that of SNYA sample. This is an indication of the formation of a solid solution, E_2SiO_5, where Y atomic sites are partially substituted by rare-earth atoms, such as Yb, Er, Dy, etc. The atomic positions refined for Y_2SiO_5 are shown in the Table 3. The atomic positions refined for E_2SiO_5 were found to be similar to that of Y_2SiO_5.

Table 3
Fractional coordinates for Y_2SiO_5

Atom	Wyckoff site	*x*	*y*	*z*
Y(1)	8f	0.501(7)	0.799(6)	0.483(7)
Y(2)	8f	0.288(4)	0.947(9)	0.671(5)
Si	8f	0.27(1)	0.43(2)	0.59(1)
O(1)	8f	0.21(2)	−0.04(5)	0.57(3)
O(2)	8f	0.02(2)	0.56(3)	0.69(2)
O(3)	8f	0.29(2)	0.24(4)	0.71(3)
O(4)	8f	0.45(2)	0.59(3)	0.70(2)
O(5)	8f	0.13(2)	0.92(4)	0.38(2)

The number in the parenthesis denotes standard deviation.

The refinement taking account three phases show good final reliability factors, calculated as defined in the literature [20]: $R_p = 13.8\%$, $R_{wp} = 18.0\%$ and $R_{exp} = 6.59\%$ for SNYA sample and $R_p = 13.8\%$, $R_{wp} = 18.0\%$ and $R_{exp} = 6.59\%$ for SNEA sample. The Bragg reliability factors calculated for each phase were: $R_B = 4.42\%$ (β-Si_3N_4), 9.37% ($Y_3Al_5O_{12}$) and 18.6% (Y_2SiO_5) for SNYA sample and $R_B = 5.55\%$ (β-Si_3N_4), 10.2% ($E_3Al_5O_{12}$) and 18.4% ($E_3Al_5O_{12}$) for SNEA sample. The phase fractions calculated in vol.% for each sample were: β-Si_3N_4 (87.6%), $Y_3Al_5O_{12}$ (7.0%) and Y_2SiO_5 (5.4%) for SNYA sample and β-Si_3N_4 (81.3%), $E_3Al_5O_{12}$ (10.1%) and E_2SiO_5 (8.6%) for SNEA sample.

3.3. Microstructure

The SEM micrographs of the sintered samples, SNYA and SNEA, are shown in Fig. 3.

The microstructures of both samples are very similar and are composed of elongated β-Si_3N_4 grains (dark region) with a grain size of about 2 μm with an aspect ratio of 6, surrounded

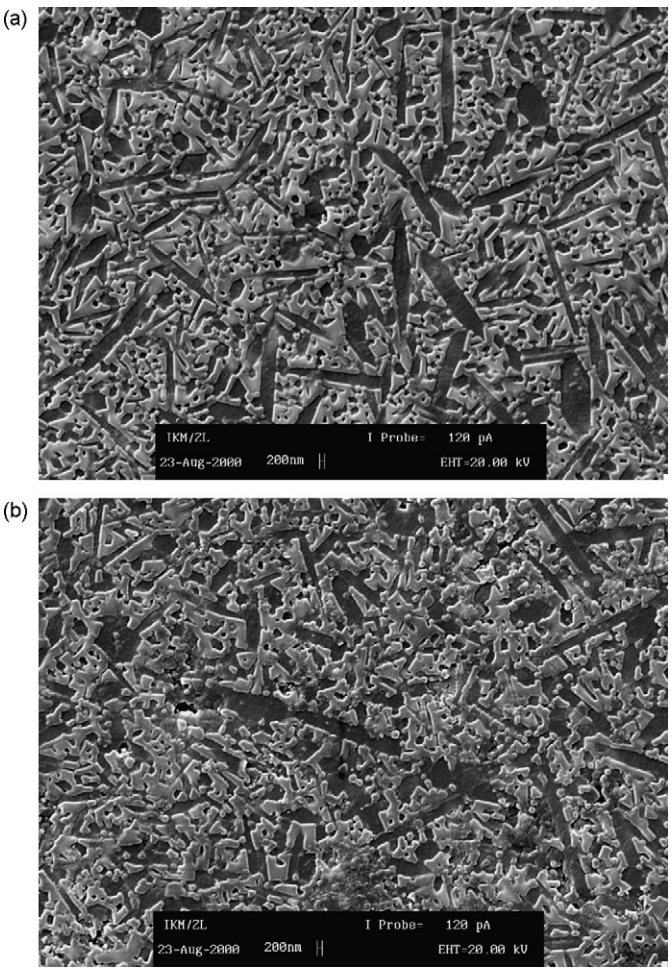

Fig. 3. SEM micrographs of the sintered samples: (a) SNYA and (b) SNEA after heat-treatment at 1400 °C for 24 h in 0.1 MPa of N_2.

by the intergranular phase (clear region). In the clear region it is not possible to identify the multiple phases probably due to low contrast exhibited by close composition of the intergranular phases.

4. Conclusions

Silicon nitride ceramics were sintered using Y_2O_3–Al_2O_3 (SNYA) or E_2O_3–Al_2O_3 (SNEA) as additive. In both samples the same phases were identified: β-Si_3N_4, $Y_3Al_5O_{12}$ and Y_2SiO_5. The crystal structures of β-Si_3N_4 formed using both additives exhibit were similar lattice parameters. In the sample SNEA it was detected the formation of solid solutions of $E_3Al_5O_{12}$ and E_2SiO_5, isostructural to respectively $Y_3Al_5O_{12}$ and Y_2SiO_5.

The similarity in the physical properties for both SNYA and SNEA samples show that the silicon nitride ceramics could be produced using E_2O_3–Al_2O_3 as an alternative sintering additive.

Acknowledgments

The authors would like to acknowledge the Brazilian Synchrotron Light Laboratory (LNLS) for permission to conduct the high-resolution X-ray measurements at the D12A-XRD1 beamline, under project #2047/03.

References

[1] F.L. Riley, Silicon nitride and related materials, J. Am. Ceram. Soc. 83 (2) (2000) 245–265.
[2] A. Bellosi, Design and process of non-oxide ceramics. Case study: factors affecting microstructure and properties of silicon nitride, in: Y.G. Gogotsi, R.A. Andreievski (Eds.), Materials Science of Carbides Nitrides and Borides, Kluwer Academic Publishers, Netherlands, 1999, pp. 285–304.
[3] A.J. Pyzik, D.R. Braman, Microstructure and properties of self-reinforced silicon nitride, J. Am. Ceram. Soc. 76 (6) (1993) 2737–2744.
[4] C. Santos, K. Strecker, S. Ribeiro, J.V.C. de Souza, O.M.M. Silva, C.R.M. Silva, α-SiAlON ceramics with elongated grain morphology using an alternative sintering additive, Mater. Lett. 58 (11) (2004) 1792–1796.
[5] K.H. Jack, Review—sialons and related nitrogen ceramics, J. Mater. Sci. 11 (1976) 1135–1158.
[6] R.M. German, Sintering Theory and Practice, John Wiley and Sons, 1996 550p.
[7] K. Strecker, R. Gonzaga, S. Ribeiro, M.J. Hoffmann, Substitution of Y_2O_3 by a rare earth oxide mixtures as sintering additive of Si_3N_4 ceramics, Mater. Lett. 45 (2000) 39–42.
[8] C. Santos, K. Strecker, S.A. Baldacim, O.M.M. Silva, C.R.M. Silva, Mechanical properties improvement related to the isothermal holding time in Si_3N_4 ceramics sintered with an alternative additive, Int. J. Refract. Met. Hard Mater. 21 (5–6) (2003) 245–250.
[9] C. Santos, S. Ribeiro, K. Strecker, C.R.M. da Silva, Substitution of pure Y_2O_3 by a mixed concentrate of rare earth oxides (CRE2O3) as sintering additive of Si_3N_4: a comparative study of the mechanical properties, J. Mater. Process. Technol. 142 (3) (2003) 697–701.
[10] C. Santos, K. Strecker, P.A. Suzuki, S. Kycia, O.M.M. Silva, C.R.M. Silva, Stabilization of (-SiAlONs using a rare-earth mixed oxide (RE2O3) as sintering additive, Mater. Res. Bull. 40 (2005) 1094–1103.
[11] K. Keller, T. Mah, T.A. Parthasarathy, Processing, mechanical properties of polycrystalline $Y_3Al_5O_{12}$ (Yttrium Aluminum Garnet), Ceramic Eng., Sci. Proc. 11 (7–8) (1990) 1122–1133.
[12] W. Kraus, G. Nolze, POWDER CELL—a program for the representation and manipulation of crystal structures and calculation of resulting X-ray powder patterns, J. Appl. Cryst. 29 (1996) 301–303.
[13] J. Rodriguez-Carvajal, Reference Guide for the Computer Program Full-Prof, Laboratoire Leon Brillouin, CEA-CNRS, Saclay, France, 1996.
[14] G. Wotting, B. Kanka, G. Ziegler, Microestructural characterization, and relation to mechanical properties of dense silicon nitride, in: S. Hampshire (Ed.), Non-Oxide Technical and Engineering Ceramics, Elsevier, London, U.K, 1986, pp. 83–96.
[15] R. Grün, The crystal structure of beta Si_3N_4; structural and stability consideration between alpha and beta—Si_3N_4, Acta Cryst. 35B (1979) 800–804.
[16] F. Euler, J.A. Bruce, Oxygen coordinates of compounds with garnet structure, Acta Cryst. 19 (1965) 971–978.
[17] PDF Files, JCPDS, International Centre for Diffraction Data, 1997.
[18] J. Wang, S. Tian, G. Li, F. Liao, X. Jing, Preparation and X-ray characterization of low temperature phases of R_2SiO_5 (R = rare earth elements), Mater. Res. Bull. 36 (2001) 1855–1861.
[19] T. Gustafsson, M. Klintenberg, S.E. Derenzo, M.J. Weber, J.O. Thomas, Lu_2SiO_5 by single-crystal X-ray and neutron diffraction, Acta Cryst. C57 (2001) 668–669.
[20] R.A. Young (Ed.), The Rietveld Method, Oxford University Press, Great Britain, 1996.